High-Q sensor based on hybridized spoof localized surface plasmons

JUN WANG,[1,2,3] ⃝ SHI-ZHUANG YAN,[1] XIANGLIN KONG,[1] RUOFENG XU,[1] AND LEI ZHAO[1,*] ⃝

[1] *School of Information and Control Engineering, China University of Mining and Technology, Xuzhou 221116, China*
[2] *Science and Technology on Antenna and Microwave Laboratory, Xidian University, Xi'an 710071, China*
[3] *State Key Laboratory of Millimeter Waves, School of Information Science and Engineering, Southeast University, Nanjing 211189, China*
*leizhao@cumt.edu.cn

Abstract: A high-Q sensor based on hybridized spoof localized surface plasmon (LSP) has proved to be advantageous in detection and sensing. The sensor is composed of three concentric inner, middle, and outer LSP structures with corrugated rings coupled with each other. Through multiple hybridizations of spoof LSP, the maximum simulated Q-factor of the sensor is up to 414, and the sensitivity is up to $1.47\,\text{GHz·RIU}^{-1}$. To validate the proposed sensor design concept, a prototype of the sensor with three layers is fabricated and measured, the measured results are in agreement with the simulated ones.

1. Introduction

Localized surface plasmon (LSP) is generated by the incident electromagnetic wave and the resonance of electrons on the surface of nanoparticles [1–3]. The characteristics of LSPs have attracted great attention of researchers and make the local surface plasmon play a very vital role in designing nonlinear optical effect, resonators, filters, sensors, and biological detection [4–10,26–31].

LSPs only exist in the optical band, which limit the application in the microwave band until Pendry et al proposed the corrugated metal cylinder structure that can support spoof localized surface plasmon [11], and Cui et al designed the ultra-thin spoof LSP structure [12] that laid the foundation of practical application in LSP. Subsequently, researchers proposed many different spoof LSP structures, such as ultra-thin corrugated metal-insulator-metal ring resonator [13], compact spoof LSPs [14], spoof LSP hybridization structure [15] and spiral hybridization LSP [16], etc. In ref. 17, a quarter mode microfluidic chemical sensor was designed, which can reduce the size with good performance. Moreover, a flexible printed microwave sensor was proposed by using a metal ring structure with corrugated grating for continuous health monitoring [18]. Compared with the traditional cavity structure, the designs of sensors based on spoof LSPs have improved quality factor. To further enhance the sensor performance, some other methods have been proposed, such as chemical sensing by adding black phosphorus and graphene [19], exponential sensors with multi-mode interference [20], and multi-factor sensors [21]. However, the complex design and high manufacturing cost limit the development. Therefore, seeking a simple design method becomes an inevitable demand.

To simplify the design, the plasmonic hybridization method was proposed by introducing subwavelength helical structure [22], which can expand the application scope of the hybrid model and provide guidance for the design of low frequency plasmonic hybridization. For reducing radiation loss, a circular plasmon resonance model was designed by compressing the Mie resonance mode, which consists a double-layer concentric inward-facing and outward-facing spoke pattern [23]. The structure can excite a trap mode with a quality factor of 104.8 while the

diameter size is only 1/20 wavelength. However, the design still has great room for improvement in quality factor. Recently, Wang et al proposed a hybrid spoof LSP sensor with high quality factor and high sensitivity, and the Q-factor of the design is up to 178 [24]. However, the complexity of the design still needs to be simplified. Therefore, how to design a spoof LSP microwave sensor with high quality factor, high sensitivity and simple structure is a challenging work.

In this paper, a multimode and high Q-factor microwave sensor based on hybridized spoof LSP is designed. The sensor is composed of three concentric inner, middle, and outer LSP structures with corrugated rings coupled with each other. Through multiple hybridization of spoof LSPs, the maximum simulated Q-factor of the sensor is up to 414, and the sensitivity is up to 1.47GHz·RIU^{-1}. For validating the proposed sensor design concept, a prototype of the sensor with three layers is fabricated and measured and the measured results have a good agreement with the simulated ones, which can be used for material detection applications.

2. Sensor design and simulation

Figure 1 shows the structure of spoof LSP sensor. The spoof LSP sensor consists of three independent metal rings with corrugated gratings printed on Rogers 5880 substrate. The substrate size is 54 mm×40 mm×0.508 mm, and the dielectric constant is 2.2. The structure with corrugated grating on the outer ring is the most common structure to support spoof LSP, which is fed by microstrip lines and partial circular coupling ring. In order to better analyze the designed sensor, the single-layer of the outer ring, the double-layers of middle ring and outer ring, and the triple-layers are analyzed respectively.
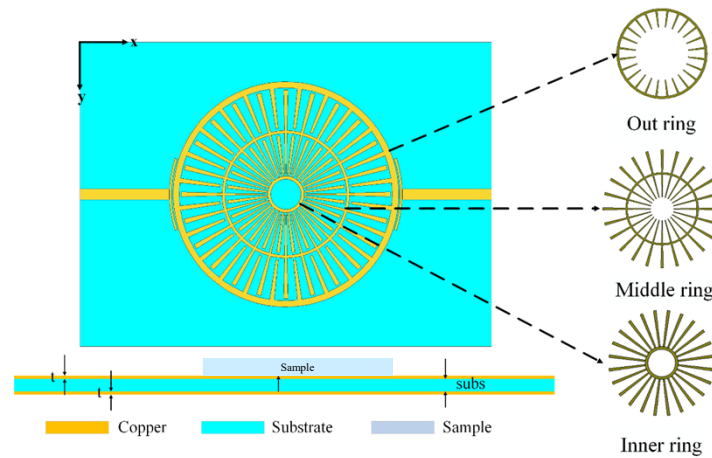

Fig. 1. The top view and side view of spoof LSP sensor

2.1. Single-layer structure of spoof LSP sensor

The S-Parameters and electric field diagrams of single-layer structure of spoof LSP sensor are shown in Fig. 2. The outer sloop LSP structure is excited by microstrip lines without sample and the resonance LSP modes are standing waves in the ring, which can be compared with microwave ring resonators and split-ring resonators (SRRs) [32]. The surface currents of the dipole modes in the LSP structure can be excited by the penetrated magnetic waves in full-wavelength resonance, and the currents mainly resonances as a pair of in-phase surface current along the periphery annular path in the two sides of the metallic structure. As shown in Figs. 2(b)-(e), four resonance points were generated at 1.71 GHz, 3.36 GHz, 4.92 GHz, and 6.24 GHz, respectively. The corresponding resonance modes of the four resonance points are dipole mode, quadrupole mode,

hexapole mode, and octupole mode, which are represented by m_1, m_2, m_3, m_4 respectively. The electric field diagrams are all taken from 0.5 mm above the vertical direction of the structure in Figs. 2(b)-(e). In the dipole mode of Fig. 2(b), the structure has positive charges on the left side and negative charges on the right. Therefore, the electric fields are oscillated in opposite phase in the left and right halves. Figs. 2(c)-(e) show multi-pairs of electric fields oscillated in opposite phase, which corresponding to quadrupole mode, hexapole mode, and octupole mode of the proposed single design. In order to demonstrate the performance of single ring spoof LSP sensors more conveniently and intuitively, sensitivity simulation tests were conducted and the quality factor of the resonant structure was calculated as well. The samples used for sensitivity testing are Rogers 5880 (ε=2.2), Rogers 4003C (ε=3.55), Rogers 3003(ε=3), ε is the dielectric constant. The test sample is a cube with the same thickness and side length as to the substrate. The simulation results are shown in Fig. 2(a). When dielectric plates with different dielectric constants are placed on the designed structure, the resonance frequencies of different resonant modes will shift, and the offset of the resonance frequency will increase with the increase of the number of modes. The sensitivity calculation is based on the octupole mode(m_4). Take this resonance point as example, when the dielectric constant of the tested object is reduced from 3.55 to 2.2, the offset of the resonant frequency is 0.12 GHz. The sensitivity can be calculated by formula (1), Δf is the offset of the resonance frequency and the refractive index Δn is equal to the square root of the relative dielectric constant ε of the sample under test. The sensitivity of the octapole mode is calculated to be $0.30\,\text{GHz·RIU}^{-1}$, while the Q factor is 79. Therefore, there is great potential for improving the performance of both sensitivity and quality factor of the single ring structure.

$$sensitivity = \frac{\Delta f}{\Delta n} \tag{1}$$

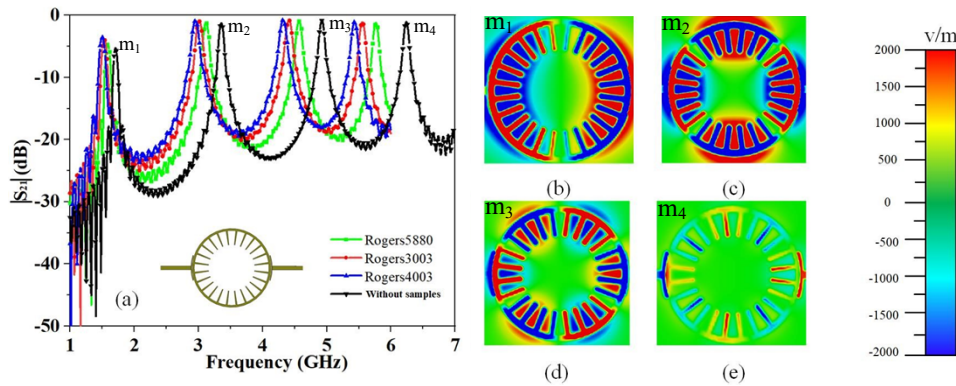$$Q = \frac{f_0}{f_{3dB}} \tag{2}$$

Fig. 2. (a) The outer ring of spoof LSP sensor and the simulated S-parameters, (b)-(e) The electric field of m_1 to m_4.

The frequency shift $\Delta\omega$ caused by the change of dielectric constant is usually proportional to the volume of the electric field intensity in the detection object. In the outer ring structure analyzed above, the electric field is only concentrated at the grating and the intensity of electric field is very low.

2.2.　Double-layers structure of spoof LSP sensor

In order to achieve a higher volume fraction of electric field in the test samples, a ring metal grating structure is added in the middle of the outer ring, which is shown in Fig. 3. This design

not only expands the contact area between the electric field and the test sample, but also further improves the electric field intensity through hybridization between the double rings. Therefore, the performance of the sensor has a great improvement.
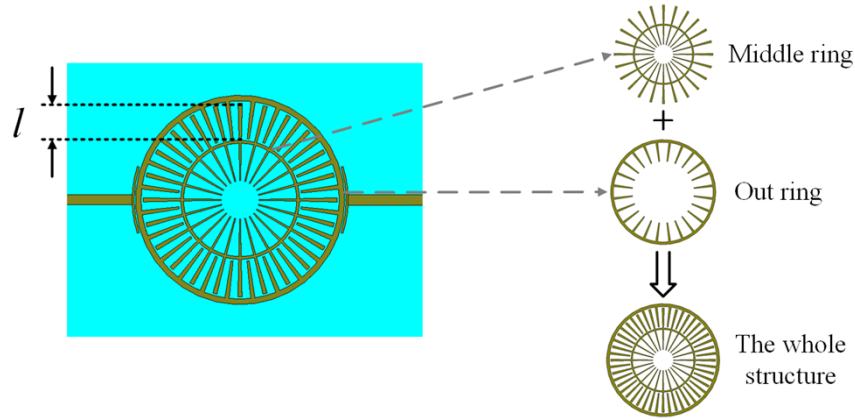

Fig. 3. Concentric spoof LSP with two layers

The metal grating structures of the outer ring and the middle ring are interlaced with each other and the length of the intersecting grating part l can be used to regulate the coupling strength of the two parts, which can be clearly seen from Fig. 4. As the S-parameter shown in Fig. 4(a), when the length of l is 5.3 mm, 4.3 mm and 3.3 mm, the resonant frequency of m_4 is 3.8 GHz, 3.96 GHz and 4.2 GHz, respectively, and the resonance intensity of the resonant point will also decrease as well. Figures 4(b)-(d) indicate that when the length of l decreases, the intensity of electric field and the range of strong electric field also decrease. In order to achieve stronger field enhancement, the length of l should be set as long as possible. Based on this analysis, the length of l is set as 5.3 mm according to the comparison results in Fig. 4.
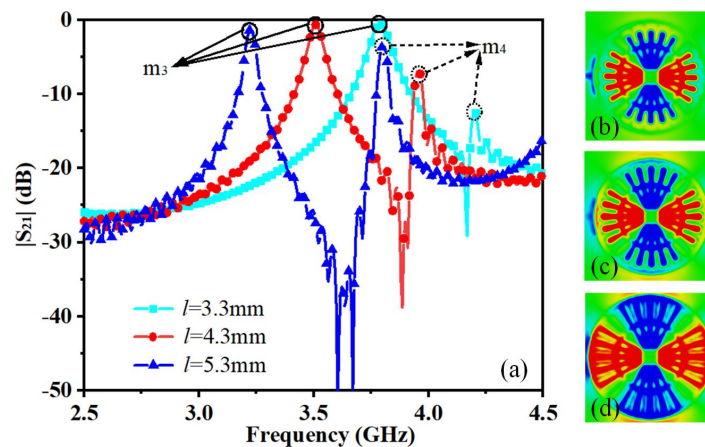

Fig. 4. The simulated results of double-layer structure with different length of l, (a) S-parameter, (b)-(d) The electric field diagram of m_4 resonance point when l increases from 3.3 mm to 5.3 mm.

Compared with single-layer spoof LSP structure, double-layer structure can generate more resonant modes and higher electric field intensity in the same frequency band which gives it an advantage in terms of sensitivity. The resonant frequencies of the double-layer structure

are respectively located at 1.65 GHz, 1.96 GHz, 3.23 GHz, 3.8 GHz, 4.65 GHz, 5.4 GHz, 5.8 GHz and 6.7 GHz. They are labeled with m_1, m_2, m_3, m_4, m_5, m_6, m_7, and m_8, respectively. Simulation results of S-Parameter and electric field are shown in Fig. 5. The electric field is taken from 0.5 mm above the metal structure. The advantages of the double-ring structure are analyzed through simulation and calculation of the sensing performance, and results are compared with the single-ring structure as well. Since the highest resonance mode that can be excited by the single ring is m_4, the comparison results of the fourth resonance point between the single-ring and the double-ring structure are taken as an example. It can be clearly seen from Fig. 2(e) and Fig. 5(e) that both the electric field intensity and the area covered by the strong electric field in the double-ring structure are much larger than that in the single-ring structure, which will improve the offset of the resonant point of the double-ring structure and thus improve the sensitivity of the structure. For a more intuitive comparison sensitivity and Q factor, Rogers 5880, Rogers 4003C and Rogers 3003 test samples are added to the double-ring structure for detection. The size and thickness of the samples used in the double-ring structure are exactly same as those in the single-ring structure.
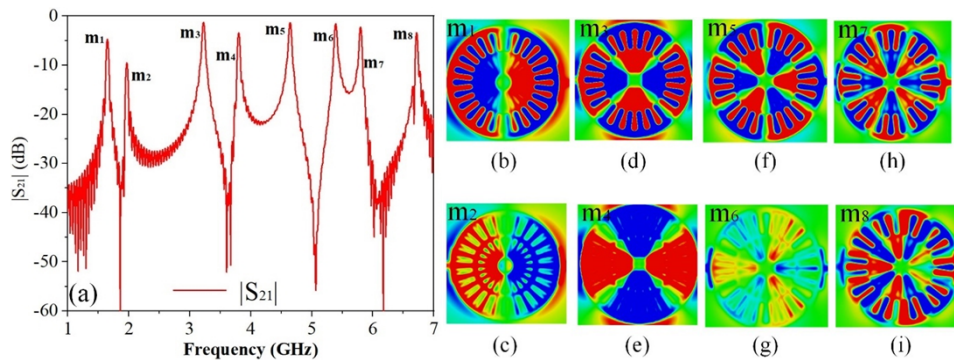

Fig. 5. Simulation results of spoof localized surface plasmon with double-layer, (a)S-parameters, (b)-(i) The diagrams of electric field in m_1-m_8.

Due to the complex mode and for better showing the sensing performance of the selected resonant point, only S-Parameter of m4 resonant point is retained and results of other modes are removed, which is shown in Fig. 6. It can be seen from the figure that the resonant frequencies are 3.80 GHz without test sample and 3.59 GHz, 3.5 GHz, 3.45 GHz with Rogers 5880, Rogers 3003 and Rogers 4003 test plates, respectively. Therefore, when the dielectric constant is reduced from 3.55 to 2.2, the offset of the resonant frequency is 0.14 GHz, and the sensitivity of the mode is 0.35 GHz·RIU^{-1}, which is higher than that of the single-layer structure. The calculated Q-factor is up to127 which is much higher than that of single layer structure (79). In addition, the double-layer structure can excite more higher modes, and the higher-order mode has higher sensitivity and quality factor than the lower-order mode. In the double-layer structure, when the dielectric constant changes from 3.55 to 2.2, the resonant frequency of mode m7 changes from 5.98 GHz to 6.26 GHz, the frequency offset is 0.28 GHz and the calculated sensitivity is 0.70GHz·RIU^{-1}, the calculated Q-factor is 165. The maximum sensitivity of double-layer structure is about 2.3 times that of single-layer structure, and the maximum quality factor is about 2.1 times that of single-layer structure.

Therefore, compared with the single-layer structure, the double-layer structure has better performance in electric field strength, sensitivity, and Q-factor. This is mainly because that the hybridization between the double-layer LSP structures makes the double-layer LSP structure have stronger electric field strength and generate higher resonance mode. The proposed dual-layer
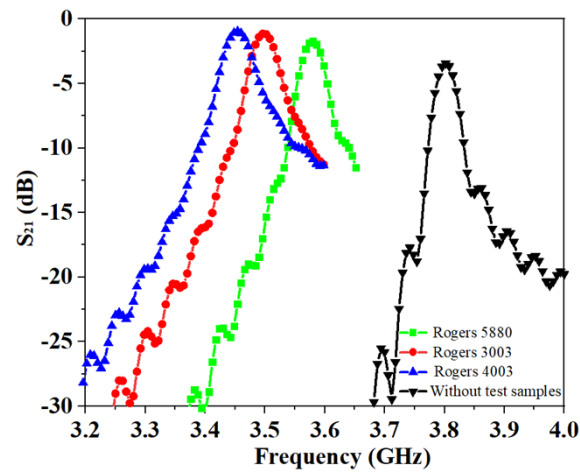
Fig. 6. The S-parameter diagram of the double-layer localized surface plasmon with the test sample added when the resonance point is m_4.

spoof LSP sensor designed has a maximum sensitivity of $0.70\,\text{GHz}\cdot\text{RIU}^{-1}$ and a maximum Q-factor of 165.

2.3. Three-layers structure of spoof LSP sensor

In order to further improve the sensing performance, an inner LSP structure is added based on the double-layer LSP structure to further improve the electric field intensity, and a higher resonant mode is excited to improve the sensitivity. The structure and detailed dimension parameters of the designed sensor are shown in Fig. 7. Rogers 5880 with the size of $54\,\text{mm}\times40\,\text{mm}\times0.508\,\text{mm}$ is used as the substrate of the sensor, the dielectric constant and the loss angle tangent are 2.2 and 0.0009 respectively. The feed port is fed by microstrip line, whose width w1 is 1.45 mm and length L1 is 11.7 mm. For the sake of better feeding, a partial ring was used at the top of the microstrip line to couple with the overall structure. The angle θ of the partial ring was 36°, the gap width w2 between the partial ring and the outermost ring structure was 0.3 mm, and the thickness of the metal was 0.018 mm. At the back of the substrate, a metal plate with the
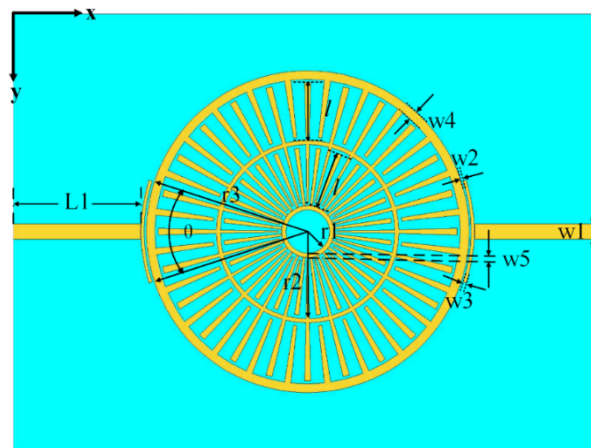

Fig. 7. The structure of spoof LSP sensor with three layers.

same size and thickness as the substrate was 0.018 mm. The radii of the three rings are set as: r1 = 14.8 mm, r2 = 8.4 mm and r3 = 2.4 mm, respectively. The length of the metal grating with grooves is 5.3 mm and the number of grooves N is 24.

Compared with the single-layer and double-layer structures, the three-layer spoof LSP structure introduced can generate higher resonant modes, and its simulation results are shown in Fig. 8. The S-parameters show that the structure has nine resonant points in the frequency band of 0-7 GHz, and the resonant frequencies are 1.64 GHz, 1.88 GHz, 3.20 GHz, 3.63 GHz, 4.61 GHz, 5.23 GHz, 5.67 GHz, 6.27 GHz, 6.63 GHz, which are labeled with m_1, m_2, m_3, m_4, m_5, m_6, m_7, m_8, and m_9, respectively. Figure 8(b) is the electric field pattern of the structure, which is taken from 0.5 mm directly above the metal structure.
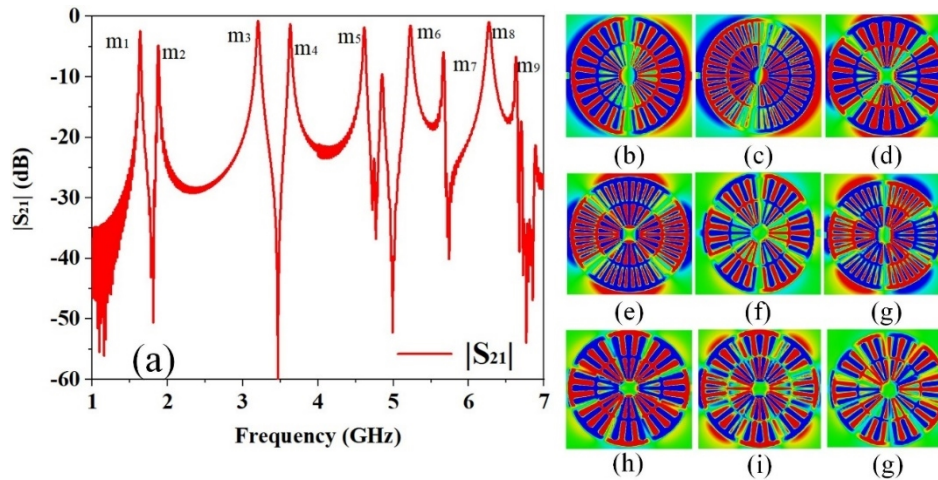

Fig. 8. The simulated results of the Triple-layer localized surface plasmon, (a)S-parameters, (b)-(g)The diagrams of electric field.
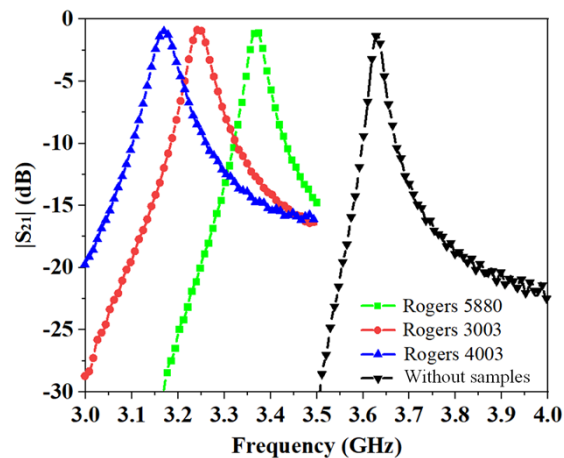

Fig. 9. The S-parameter diagram of the three-layer localized surface plasmon with the test sample added when the resonance point is m_4

The resonant mode used for comparison is the same as above, which is still the m_4 resonant point. The tested samples are still using Rogers 5880, Rogers 4003C and Rogers 3003 plates

whose size and thickness are exactly same as the above, the simulation results are shown in Fig. 9. In order to avoid the interference of other resonant mode data, the parameters of other modes are removed in Fig. 9, and only the S-parameters of the m_4 resonant point are shown. The resonant frequencies are 3.63 GHz, 3.37 GHz, 3.24 GHz and 3.20 GHz, when the test samples are not added and the Rogers 5880, Rogers 3003 and Rogers 4003 are added respectively. When the dielectric constant is reduced from 3.55 to 2.2, the offset of the resonant frequency is 0.2 GHz and the sensitivity of the mode is 0.50 GHz·RIU^{-1}, which is higher than 0.30 GHz·RIU^{-1} of the single layer structure and 0.35 GHz·RIU^{-1} of the double layer structure. The Q-factor is 137, which is larger than 127 of the double-layer structure and much larger than 79 of the single-layer structure.

In addition, the three-layer structure can also excite higher-order modes, which have higher sensitivity and Q-factor compared with lower-order modes. In order to compare the advantages, the sensing performance of the m_4 resonant point and the highest resonant frequency of each structure are listed more intuitively in Table 1. In the three-layer structure, when the dielectric constant is reduced from 3.55 to 2.2, the resonant frequency of the highest resonant mode m_9 changes from 5.28 GHz to 5.87 GHz, the offset of the resonant frequency is 0.59 GHz, and the sensitivity calculation result is 1.47 GHz·RIU^{-1}, and the Q-factor calculation result is 414. Therefore, the maximum sensitivity of three-layer structure is about 4.9 times and 2.1 times of that of single-layer and double-layer structure, and the quality factor is about 5.2 times and 2.5 times of that of single-layer and double-layer structure, respectively. Therefore, compared with the single-layer and double-layer structures, the three-layer structure has a great improvement in terms of sensitivity and Q-factor, which proves the rationality of the three-layer structure design.

Table 1. Comparison of Single-Layer, Double-Layer and Three-Layer Structures

Structure type	Resonance offset (GHz)	Sensitivity (GHz·RIU^{-1})	Q-factor
Single layer	0.12 (m_4)	0.30	79
Double layer	0.14 (m_4)	0.35	127
	0.28 (m_7)	0.70	165
Three layer	0.20 (m_4)	0.50	137
	0.59 (m_9)	1.47	414

3. Experimental verification

In order to verify the correctness of the simulation results, a three-layer sensor sample is fabricated and measured. Figure 10(a)-(c) are the diagram of the sensor, the sensor with the test sample, and the test sample with different dielectric constant. The test samples are fixed to the surface of the sensor through the plastic clip. It should be noted that the test amplitude of the resonant peak is lower than the simulated ones, which is caused by some unpredictable system or material loss. Figure 11(a) shows the S-parameter diagram of the sensor without test sample. As can be seen from the figure, the measured results and simulated results slightly deviate in terms of resonant frequency, and the resonance strength is slightly lower than the simulation results, due to the SMA adapter and measured environment increasing the loss. In addition, the manufacture technology problem may also be one of the reasons for the deviation of the results, which are not considered in the simulation design, but overall, the two parts are in good agreement. Figure 11(b) shows the comparison of simulated and measured results after adding test samples with different permittivity. It can be seen from the figure that when the permittivity changes, the resonant frequency will shift, and the offset will increase with the increase of the number of modes. The measured and simulated results are basically consistent, and the difference between the results

may be affected by the manufacture technology problem and the fitting degree between the sample to be tested and the sensor.
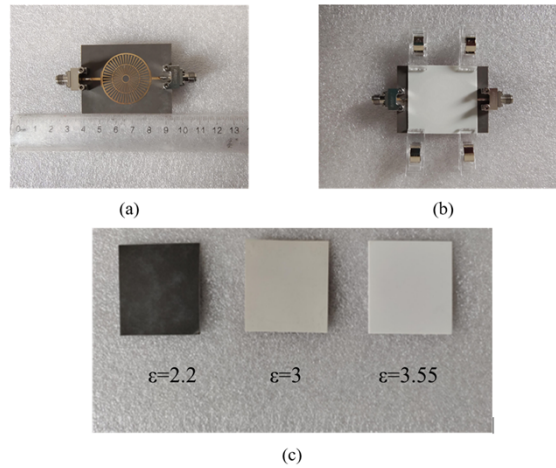

Fig. 10. Photo of the fabricated three-layer sensor prototype, (a)The sensor, (b)The sensor with sample, (c)The three samples with different permittivities for sensor detection
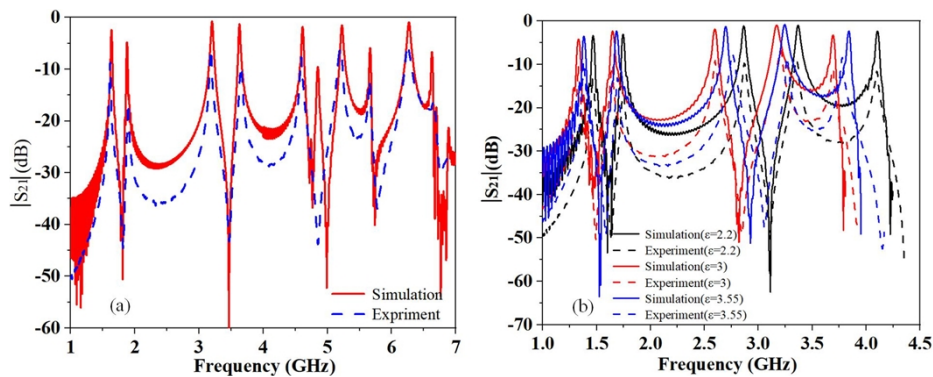

Fig. 11. The simulated and measured S-parameter, (a)without test samples, (b)with test samples.

Table 2 lists the performance of this design and the sensors based on local surface plasmon in recent years. In [23], a sensor composed of concentric mutually coupled corrugated ring LSPs structure was designed. Although it has high sensitivity and the Q-factor is up to 178, the performance depends on the subsequent processing of a hybrid resolution algorithm, and the process is complicated. Article [24] proposed a hybrid plasma resonator through electromagnetic mode interference and improves the quality factor by 3.4 times through the hybrid mode, however, this sensor still needs to be further improved in terms of sensitivity and quality factor. In [25], a planar texture metal disk LSPs structure that can effectively excite and enhance multipole resonance through the trumpet groove line is proposed. The quality factor of this structure is up to 336, but there is still a large room for improvement in sensitivity. Through comprehensive comparison, the sensor designed in this chapter has advantages in sensitivity and quality factor.

Table 2. Simulated Performance Comparison of Existing Sensor Structures

Reference	Sensitivity (GHz·RIU^{-1})	Q-factor
[12]	0.9	82
[23]	1.49	178
[24]	1.1	153
[25]	0.825	336
Our work	1.47	414

4. Conclusion

In this paper, a sensor based on spoof local surface plasmons is presented which is composed of three independent plasmons. The proposed design is introduced by analyzing the single-layer, the double-layers and the three-layers structures respectively. Through research on the effect of the coupled grating length between outer and middle layers, we explained the reasons for the performance improvement of multi-layer LSPs sensor. The simulation results show that the sensitivity of the three-layer structure is 1.47 GHz·RIU^{-1} and it is about 4.9 times and 2.1 times of that of single-layer structure and double-layer structure, the Q-factor is 414, which is about 5.2 times and 2.5 times of that of single-layer structure and double-layer structure, respectively. A prototype of the sensor is fabricated and measured, and the measured results have a good agreement with the simulated ones, verifying the correctness of the design.

Disclosures. The authors declare no conflicts of interest.

Data availability. No data were generated or analyzed in the presented research.

References

1. K. A. Willets and D. R. P. Van, "Localized surface plasmon resonance spectroscopy and sensing," Annu. Rev. Phys. Chem. **58**(1), 267–297 (2007).
2. K. M. Mayer and J. H. Hafner, "Localized surface plasmon resonance sensors," Chem. Rev. **111**(6), 3828–3857 (2011).
3. Z. Gao, L. Wu, F. Gao, *et al.*, "Spoof plasmonics: from metamaterial concept to topological description," Adv. Mater. **30**(31), 1706683 (2018).
4. A. Degiron and T. Ebbesen, "Analysis of the transmission process through single apertures surrounded by periodic corrugations," Opt. Express **12**(16), 3694–3700 (2004).
5. P. B. Catrysse and S. Fan, "Near-complete transmission through subwavelength hole arrays in phonon-polaritonic thin films," Phys. Rev. B **75**(7), 075422 (2007).
6. B. J. Yang, Y. J. Zhou, and Q. X. Xiao, "Spoof Localized Surface Plasmons in Corrugated Ring Structures Excited by Microstrip Line," Opt. Express **23**(16), 21434–21442 (2015).
7. J. H. Zou, X. Q. Yang, H. Y. Li, *et al.*, "A Liquid Level Positioning System for Non-Metal Containers Based on Localized Spoof Surface Plasmon," IEEE Sens. J. **24**(6), 7729–7739 (2024).
8. Z. Li, L. Liu, C. Gu, *et al.*, "Multi-band Localized Spoof Plasmons with Texturing Closed Surfaces," Appl. Phys. Lett. **104**(25), 101063 (2014).
9. C. C. Luo and L. Chen, "Highly Sensitive and Tunable Absorption-Induced Transparency for Terahertz Fingerprint Sensing with Spoof Surface Plasmon Polaritons," IEEE Sens. J. **24**(11), 17686–17692 (2024).
10. Z. B. Yang, D. F. Guan, X. Huang, *et al.*, "Compact and Wideband Octuple-Mode Filter Based on Hybrid Substrate Integrated Waveguide and Spoof Localized Surface Plasmon Structure," IEEE Trans. Circuits Syst. **67**(11), 2377–2381 (2020).
11. A. Pors, E. Moreno, L. Martin-Moreno, *et al.*, "Localized Spoof Plasmons Arise while Texturing Closed Surfaces," Phys. Rev. Lett. **108**(22), 223905 (2012).
12. X. Shen and T. J. Cui, "Ultrathin plasmonic metamaterial for spoof localized surface plasmons," Laser Photonics Rev. **8**(1), 137–145 (2014).

13. Y. J. Zhou, Q. X. Xiao, and B. J. Yang, "Spoof Localized Surface Plasmons on Ultrathin Textured MIM Ring Resonator with Enhanced Resonances," Sci. Rep. **5**(1), 14819 (2015).
14. D. Bao, K. Z. Rajab, W. X. Jiang, *et al.*, "Experimental Demonstration of Compact Spoof Localized Surface Plasmons," Opt. Lett. **41**(23), 5418–5421 (2016).
15. D. Bao, Q. Cheng, W. X. Jiang, *et al.*, "Concentric designer plasmon hybridization in deep subwavelength metamaterial resonator," Appl. Phys. Lett. **115**(12), 121103 (2019).
16. Z. Gao, F. Gao, Y. Zhang, *et al.*, "Complementary structure for designer localized surface plasmons," Appl. Phys. Lett. **107**(19), 191103 (2015).
17. R. L. Shao, Y. J. Zhou, and L. Yang, "Quarter-mode Spoof Plasmonic Resonator for a Microfluidic Chemical Sensor," Appl. Opt. **57**(28), 8472–8477 (2018).
18. L. Dai, H. Zhao, Z. Zhao, *et al.*, "Flexible and Printed Microwave Plasmonic Sensor for Noninvasive Measurement," IEEE Access **8**, 163238–163243 (2020).
19. Y. Singh, M. K. Paswan, and S. K. Raghuwanshi, "Sensitivity Enhancement of SPR Sensor with the Black Phosphorus and Graphene with Bi-layer of Gold for Chemical Sensing," Plasmonics **16**(5), 1781–1790 (2021).
20. S. Taue, H. Daitoh, and H. Fukano, "Sensitivity enhancement of fiber-optic refractive index sensor based on multimode interference with gold nanoparticles," Jpn. J. Appl. Phys. **54**(4S), 04DL07 (2015).
21. X. Sun, H. Du, X. Dong, *et al.*, "Simultaneous Curvature and Temperature Sensing Based on a Novel Mach-Zehnder Interferometer," Photonic Sens. **10**(2), 171–180 (2020).
22. J. J. Zhang, S. A. Maier, and T. J. Cui, "Spoof plasmon hybridization," Laser Photonics Rev. **11**(1), 1600191 (2017).
23. X. Zhang and T. J. Cui, "Deep-Subwavelength and High-Q Trapped Mode Induced by Symmetry-Broken in Toroidal Plasmonic Resonator," IEEE Trans. Antennas Propagat. **69**(4), 2122–2129 (2021).
24. J. P. Wang, J. J. Zhang, H. Gao, *et al.*, "Mixed-Resolution High-Q Sensor Based on Hybridized Spoof Localized Surface Plasmons," Front. Phys. **10**, 850186 (2022).
25. X. Zhang, R. T. Yan, and T. J. Cui, "High-FoM Resonance in Single Hybrid Plasmonic Resonator via Electro-Magnetic Modal Interference," IEEE Trans. Antennas Propagat. **68**(8), 6447–6451 (2020).
26. X. X. Qian, J. Y. Bao, and J. Z. Yong, "Spoof localized surface plasmons and Fano resonances excited by flared slot line," J. Appl. Phys. **118**(23), 233112 (2015).
27. Y. Shen, N. Chen, G. Dong, *et al.*, "Manipulating Multipole Resonances in Spoof Localized Surface Plasmons for Wideband Filtering," Opt. Lett. **46**(7), 1550–1553 (2021).
28. X. Zhang and T. J. Cui, "Single-Particle Dichroism Using Orbital Angular Momentum in a Microwave Plasmonic Resonator," ACS Photonics **7**(12), 3291–3297 (2020).
29. J. H. Zou, X. Q. Yang, H. Y. Li, *et al.*, "A Wireless Non-Metallic Pipeline Liquid Level Sensor Based on Spoof Surface Plasmon Polaritons," IEEE Sens. J. **24**(6), 7761–7769 (2024).
30. Y. R. Zhang, H. Hu, F. J. García-Vidal, *et al.*, "Reconfigurable Exceptional Point-based Sensing with 0.001λ Sensitivity Using Spoof Localized Surface Plasmons," Adv. Photon. Nexus **3**(05), 056004 (2024).
31. X. H. Li, L. L. Liu, Y. R. Zhang, *et al.*, "Hybridization of Localized Spoof Plasmonic Skyrmions and its Application in Micro-displacement Sensing," Adv. Opt. Mater. **12**, 1 (2024).
32. K. Chang, *Microwave Ring Circuits and Antennas*. Wiley: New York (1996)